Role of ARID1A in epithelial-mesenchymal transition in breast cancer and its effect on cell sensitivity to 5-FU

TANGSHUN WANG*, XIANG GAO*, KEXIN ZHOU, TAO JIANG, SHUANG GAO, PENGZHOU LIU, XIMENG ZUO and XIAOGUANG SHI

Department of General Surgery, Dongzhimen Hospital, Beijing University of Chinese Medicine, Beijing 100700, P.R. China

Received December 17, 2019; Accepted July 21, 2020

DOI: 10.3892/ijmm.2020.4727

Abstract. The loss of function mutation of AT-rich interactive domain 1A (ARID1A) often occurs in patients with breast cancer. It has been found that ARID1A knockout can enhance both the migratory activity of renal carcinoma cells and their sensitivity to therapeutic drugs by promoting epithelial-mesenchymal transition (EMT); however, its mechanisms of action in breast cancer remain unclear. In the present study, immunohistochemistry and reverse transcription-quantitative polymerase chain reaction (RT-qPCR) revealed that the expression of ARID1A in breast cancer tissues was significantly lower than that in paracancerous tissues, and patients with a low ARID1A expression had a lower survival rate. ARID1A was expressed at low levels in breast cancer cells. In addition, siRNA targeting ARID1A (siARID1A) and ARID1A overexpression vector were transfected into MCF7 and MDA-MB-231 cells, respectively. Proliferation assay revealed that ARID1A silencing increased cell viability and partially reversed the inhibitory effects of 5-fluorouracil (5-FU) on the MCF7 cells, while ARID1A overexpression exerted an opposite effect on the MDA-MB-231 cells. ARID1A silencing promoted proliferation, migration, invasion and angiogenesis, and partly reversed the inhibitory effects of 5-FU on cell biological behaviors, while the overexpression of ARID1A further enhanced the inhibitory effect of 5-FU on the cells. Furthermore, ARID1A regulated the migration and invasion of breast cancer cells through EMT. On the whole, the findings of the present study demonstrate that ARID1A exerts an antitumor effect on breast cancer, and its overexpression can enhance the sensitivity of breast cancer cells to 5-FU.

Correspondence to: Dr Xiaoguang Shi, Department of General Surgery, Dongzhimen Hospital, Beijing University of Chinese Medicine, 5 Haigangcang, Dongcheng, Beijing 100700, P.R. China
E-mail: shixiaog_xguang@163.com

*Contributed equally

Abbreviations: ARID1A, AT-rich interactive domain 1A; EMT, epithelial-mesenchymal transition; RT-qPCR, reverse transcription-quantitative polymerase chain reaction; WB, western blot; CCK-8, Cell Counting kit 8; 5-FU, 5-fluorouracil; TIMP-2, tissue inhibitor of metalloproteinases-2; GDF15, growth differentiation factor 15; DMEM, Dulbecco's modified Eagle's medium; PVDF, polyvinylidene fluoride

Key words: AT-rich interactive domain 1A, breast cancer, epithelial-mesenchymal transition, 5-fluorouracil

Introduction

Breast cancer is a common type of cancer worldwide. Although some progress has been made in the treatment of breast cancer, the disease is still ranked as the second most prevalent leading cause of cancer-related mortality among females (1-3). The 5- and 10-year survival rates of patients with metastatic breast cancer are relatively low and no marked improvements in these rates have been noted over past 20-30 years; approximately 10% of breast cancer cases exhibit local recurrence, which severely affects the prognosis of patients (4). Therefore, it is of utmost importance to identify and develop effective measures with which to inhibit the metastasis of breast cancer cells. It is also critical to understand the pathogenesis of breast cancer and the expression levels of related molecules so as to develop molecular therapies which may be used to inhibit metastasis.

In recent years, an increasing number of studies have found that the differential expression of genes is of great significance to the occurrence and development of diseases, which also helps to clarify the molecular mechanisms related to diseases (5-7). Jensen *et al* in 2018 indicated that tissue inhibitor of metalloproteinases-2 (TIMP-2) can alter the transformation of epithelial cells to mesenchymal cells, and inhibit the growth, invasion and metastasis of breast cancer (8). According to the study by Raoof *et al* in 2019, in non-small lung cancer, the double blocking of EGFR and FGFR may help to prevent and overcome the occurrence of EMT-associated acquired drug resistance (9). In another study, growth differentiation factor 15 (GDF15) was expected to be a novel prognostic indicator for colorectal cancer, which may play a role in promoting the metastasis of colorectal cancer by activating EMT (10).

AT-rich interactive domain 1A (ARID1A) is located in the chromosome 1p36 region (11), and has been found to mutate in various types of cancer, such as ovarian cancer (12), endometrial cancer (13), gastric cancer (14) and pancreatic cancer (15). In addition, ARID1A mutations are associated with an increased immune activity in gastrointestinal cancer (16). It

has been reported that partial loss of ARID1A expression is related to unfavorable outcome of patients with breast cancer (17). Epithelial-mesenchymal transition (EMT) plays an important role in cancer development and progression (18). Somsuan *et al* found in 2019 that ARID1A knockout promoted EMT in cells, which was characterized by an increased fusiform index and stromal markers, decreased epithelial markers, and enhanced renal cell migration activity and drug resistance (19). Wilson *et al* in 2019 also indicated that the abnormal endometrial tissue diffusion was closely related to the increase in EMT-related gene expression induced by ARID1A deletion (20). Therefore, the role of ARID1A in the inhibition of EMT is worthy of attention. Moreover, whether ARID1A also plays a role in breast cancer by intervening in the EMT process has attracted research interests. Therefore, the present study conducted experiments to exmaine the role of ARID1A in breast cancer, in order to provide some basic referential strategies for the targeted treatment of breast cancer in clinical practice.

Materials and methods

Patient samples and patient survival rate. A total of 90 samples of breast cancer tissues and their matched adjacent tissues were collected from 90 patients aged between 30 and 50 years, who were diagnosed with breast cancer at Dongzhimen Hospital, Beijing University of Chinese Medicine from January, 2013 to January, 2014. The patients were divided into 2 groups according to the median expression level of ARID1A, and their 5-year survival rates were calculated. Approval for the study was obtained from the Dongzhimen Hospital Ethics Committee (approval no. CH201309270). Written informed consent was obtained from each patient. The demographics data of the patients are presented in Table I.

Cells and cell culture. Non-cancerous breast cells MCF-10A and breast cancer cell lines, including BT20, BT474, T-47D, MCF7, MDA-MB-231, MDA-MB-453 were acquired from the American Type Culture Collection (ATCC). Dulbecco's modified Eagle's medium (DMEM) (GE Healthcare) supplemented with 10% FBS (Gibco; Thermo Fisher Scientific, Inc.), 100 μg/ml streptomycin and 100 U/ml penicillin was used to culture the cells. The DMEM was maintained in a humidified atmosphere at 37˚C with 5% CO_2.

Transfection, reagent treatment and grouping. ARID1A siRNA (siARID1A; 5'-GGAGAUUGGUGGAUUGACUTT-3') and scrambled siRNA (siNC; 5'-UUCUCCGAACGUGUCACG UTT-3') were purchased from Santa Cruz Biotechnology, Inc. The pCMV6-XL4 and pCMV6-XL4-ARID1A (cat. no. SC303719) vectors were obtained from OriGene Technologies, Inc., and pCMV6-XL4 was used as a negative control (NC). For transfection, the MCF7 cells were transfected with 50 nM siNC or 50 nM siARID1A, while the MDA-MB-231 cells were transfected with 100 ng pCMV6-XL4-ARID1A or 100 ng NC. Cell transfection was performed using Lipofectamine 2000 (Invitrogen; Thermo Fisher Scientific, Inc.) according to the manufacturer's instructions. The cells were incubated in DMEM for 48 h at 37˚C prior to all subsequent functional investigations. Following transfection, the cells were treated with 5-fluorouracil (5-FU; 5, 10, 20, 40 and 80 μg/ml) for 24 h, which was purchased from Harbin Pharmaceutical Group.

In order to examine the effects of 5-FU on breast cancer cell viability and ARID1A expression, the groups were set as follows: The control group (untreated cells), siNC or NC group (cells transfected with siNC or NC), siARID1A or ARID1A group (cells transfected with siARID1A or pCMV6-XL4-ARID1A), 5-FU + siNC or NC group (cells transfected with siNC or NC and treated with 5, 10, 20, 40 and 80 μg/ml 5-FU), 5-FU + siARID1A or ARID1A group (cells transfected with siARID1A or pCMV6-XL4-ARID1A and treated with 5, 10, 20, 40 and 80 μg/ml 5-FU). In order to explore the function of ARID1A in breast cancer cells, the main groups in the present study were set as follows: siNC or NC group, siARID1A or ARID1A group, 5-FU + siNC or NC group (cells transfected with siNC or NC and treated with 40 μg/ml 5-FU), 5-FU + siARID1A or ARID1A group (cells transfected with siARID1A or pCMV6-XL4-ARID1A and treated with 40 μg/ml 5-FU).

Immunohistochemistry. A tissue microarray (TMA) slide set containing duplicate or triplicate 0.6-mm cores from the 90 samples of breast cancer tissues and their matched adjacent tissues from the same surgical resection specimens was used. The immunohistochemical staining of ARID1A was performed by TMA staining as follows: The mouse monoclonal anti-ARID1A antibody (sc-81193; Santa Cruz Biotechnology, Inc.) was diluted at 1/30 in blocking solution, and the primary antibody was incubated with the samples for overnight at 4˚C. The bound antibody was detected with 2 μg/ml goat anti-mouse biotin-conjugated secondary antibodies (cat. no. ab6789; 1:2,000; Abcam). Subsequently, the epithelial cells were evaluated by 2 independent observers, who were selected to read the slides in a blinded manner. The staining results were observed under a light microscope (BX53; Olympus Corporation; magnification, x200). The staining intensity was classified as 0 (negative), 1 (weak), 2 (moderate) and 3 (strong), the scores 0 and 1 were defined as low, and the scores 2 and 3 were defined as high.

Reverse transcription-quantitative polymerase chain reaction (RT-qPCR). For RT-qPCR, 10 μg of total RNA were extracted using TRIzol reagent (Invitrogen; Thermo Fisher Scientific, Inc.), and cDNA was then synthesized using oligodT and SuperScript II reverse transcriptase (Invitrogen; Thermo Fisher Scientific, Inc.). The amplification of the RT-qPCR reaction was conducted using a SYBR Premix Ex Taq kit (Takara Bio, Inc.) in the 7500 Real-time PCR system (Applied Biosystems). PCR commenced with an initial DNA denaturation step (at 95˚C for 3 min), followed by 30 cycles (denaturation at 95˚C for 30 sec, annealing at 60˚C for 30 sec, extension at 72˚C for 30 sec). The result of mRNA levels were normalized to GAPDH. PCR results were calculated using the $2^{-\Delta\Delta Cq}$ method (21), as previously described. The specific primers used are presented in Table II.

Cell proliferation assay. Following transfection, the breast cancer cells ($2x10^4$/well) in each group were plated in 96-well plates and incubated for 24 h at 37˚C. Subsequently, 10 μl of CCK-8

Table I. Association between ARID1A expression and the clinicopathological characteristics of patients with breast cancer.

Variables	No. of patients	ARID1A expression		P-value
		Negative	Positive	
Total	90	45	45	
Age (years)		52.6±10.8	53.3±12.8	0.780
TNM stage				0.003
I	27	9	18	
II	29	12	17	
III	34	24	10	
Grade				0.660
1 or 2	58	28	30	
3	32	17	15	
Tumor size				0.656
≤ cm	27	14	13	
>2, ≤5 cm	30	13	17	
>5 cm	33	18	15	
Lymph node status				0.003
Negative	40	13	27	
Positive	50	32	18	

ARID1A, AT-rich interactive domain 1A.

Table II. Sequences of primers used for RT-qPCR.

Gene	Forward (5'-3')	Reverse (5'-3')
ARID1A	TCTTGCCCATCTGATCCATT	CCAACAAAGGAGCCACCAC
E-Cadherin	TGCCCAGAAAATGAAAAAGG	GTGTATGTGGCAATGCGTTC
N-Cadherin	CCATCACTCGGCTTAATGGT	ACCCACAATCCTGTCCACAT
Vimentin	GACAATGCGTCTCTGGCACGTCTT	TCCTCCGCCTCCTGCAGGTTCTT
VEGF	TACCTCCACCATGCCAAGTG	ATGATTCTGCCCTCCTCCTTC
Cyclin D1	GGATGCTGGAGGTCTGCGA	AGAGGCCACGAACATGCAAG
Bcl-2	TTGTGGCCTTCTTTGAGTTCGGTG	GGTGCCGGTTCAGGTACTCAGTCA
Bax	CCTGTGCACCAAGGTGCCGGAACT	CCACCCTGGTCTTGGATCCAGCCC
GAPDH	TGCCAAATATGATGACATCAAGAA	GGAGTGGGTGTCGCTGTTG

ARID1A, AT-rich interactive domain 1A; VEGF, vascular endothelial growth factor.

solution (Dojindo Molecular Technologies, Inc.) were added to each well to incubate the cells for 1 h at 37˚C. The absorbance at a wavelength of 450 nm was measured using a microtiter plate (Thermo LabSystems; Thermo Fisher Scientific, Inc.).

Cell apoptosis assay. For the analysis of cell apoptosis, the breast cancer cells in each group were collected and stained with 10 μl of Annexin V-fluorescein isothiocyanate (Annexin V; Thermo Fisher Scientific, Inc.) and 5 μl of propidium iodide (PI) according to the manufacturer's instructions, and the solution was then incubated at room temperature for 15 min. The percentage of Annexin V/PI-positive cells was quantified using a FACScan flow cytometer (BD Biosciences).

Cell cycle assay. For the analysis of the cell cycle, the breast cancer cells were collected, and further fixed using 70% ice-cold ethanol at 4˚C for 1 h. The cells were then washed once with PBS. Subsequently, the breast cancer cells were incubated with RNase (0.5 mg/ml) in PBS for 1 h at 37˚C, followed by incubation with PI for 30 min at 25˚C in the dark. The cell cycle was analyzed by FACS (BD Biosciences) at 488 nm.

Western blot (WB) analysis. The breast cancer cells were lysed with ice-cold lysis buffer and the protein concentration was calculated with a BCA Protein Assay kit (Pierce; Thermo Fisher Scientific, Inc.). Equal amounts of protein were separated by

10% SDS-PAGE and transferred onto a polyvinylidene fluoride (PVDF) membrane. The membrane was then blocked using 5% non-fat milk for 1 h and incubated with the following primary antibodies overnight at 4˚C: ARID1A (1:2,000, 242 kDa, ab242377), E-cadherin (1:10,000, 97 kDa, ab40772), N-cadherin (1:1,000, 130 kDa, ab18203), Vimentin (1:1,000, 54 kDa, ab92547), vascular endothelial growth factor (VEGF; 5-10 μg/ml, 21 kDa, ab1316), cyclin D1 (1:10,000, 34 kDa, ab134175), Bcl-2 (1:2,000, 26 kDa, ab59348), Bax (1:2,000, 21 kDa, ab32503) (all from Abcam). The secondary goat anti-mouse IgG H&L (HRP) (1:2,000, ab205719) and goat anti-rabbit IgG H&L (HRP) (1:2,000, ab205718) antibodies (both from Abcam) were then used to incubate the membrane for 1 h at room temperature. Image-Pro Plus 6.0 software (Media Cybernetics, Inc.) was used to analyze protein expression. GAPDH (1:10,000, 36 kDa, ab181602; Abcam) was used as an internal control.

Wound healing migration assay. For the determination of cell migration, the breast cancer cells ($1x10^5$/well) were inoculated to 24-well plates with DMEM. An equally wide single scratch was made using 10 μl pipette tip from the top to the bottom of the culture plates when the cells of each group grew to reach 70% confluence. The debris was removed with PBS and added serum-free DMEM. Images of the cells were captured immediately after the scratch defect was made and at 24 h following incubation at 37˚C by using a light microscope (magnification, x100; Nikon Corporation).

Cell invasion assay. Transwell chambers were used to assess cell invasion. For cell invasion assay, the cells ($3x10^5$/ml) were cultured in serum-free medium. The cells were then added to the upper chamber precoated with Matrigel matrix (BD Biosciences), and medium containing 10% FBS was added to the lower chamber. Following incubation for 24 h at 37˚C, cells remaining on the surface of the upper chamber were removed with a cotton swab. The invading cells were fixed with 4% paraformaldehyde for 15 min at room temperature, and then stained with 0.1% crystal violet solution for 20 min at room temperature. Images were obtained under a light microscope (magnification, x100; Nikon Corporation) and the number of migrated cells was calculated using ImageJ software 1.8.0 (National Institutes of Health).

Tube formation assay. The breast cancer cell culture medium was changed to serum-free DMEM medium for 48 h, and the medium was then collected, centrifuged (1,000 x g, 10 min, 4˚C) and filtered to obtain tumor-conditioned medium. Subsequently, 50 μl of ice-cold BD Matrigel matrix (BD Biosciences) was added to a 24-well plate and incubated for 30 min at 37˚C. HUVECs (cat. no. PCS-100-010; ATCC) in 100 μl of conditioned medium were then added to the wells. Following incubation at 37˚C for 4 h, the wells were examined using an Olympus CKX41 microscope (Olympus Corporation). Images were then captured with an Olympus DP20-5 digital camera (Olympus Corporation) and the capillary tubes in the images were counted using ImageJ software 1.8.0 (National Institutes of Health).

Statistical analysis. The experimental data are expressed as the means ± standard deviation and analyzed using SPSS 20.0 software (SPSS, Inc.). The data in presented in Table I were analyzed using the Chi-squared test and rank sum test. The Student t-test was used to analyze differences between 2 groups, and one-way ANOVA was used to analyze differences between >2 groups followed by the Bonferroni test. The Kaplan-Meier method with the log rank test was adopted to compare the survival rates in the 2 groups. $P<0.05$ was considered to indicate a statistically significant difference.

Results

ARID1A exhibits a low expression in breast cancer. In order to examine the expression of ARID1A in breast cancer, its expression in breast cancer tissues (n=3) and their matched adjacent tissues (n=3) was analyzed by immunohistochemistry, and the results revealed that ARID1A exhibited a lower expression in the cancer tissues than in the adjacent tissues (Fig. 1A). Moreover, the staining intensity in adjacent tissue no. 1 was higher than that in adjacent tissue no. 2, but lower than that in adjacent tissue no. 3; among the 3 cancer tissues, the staining intensity in cancer tissue no. 1 was lowest and that in cancer tissue no. 3 was the highest (Fig. 1A). RT-qPCR was then performed to examine the mRNA expression of ARID1A in these tissues, and the results obtained were similar to those obtained by immunohistochemistry (Fig. 1B). Subsequently, the levels of ARID1A in MCF-10A and breast cancer cell lines, including BT20, BT474, T-47D, MCF7, MDA-MB-231, MDA-MB-453, were compared and the results indicated that ARID1A was expressed at low levels in the breast cancer cell lines compared with the normal MCF-10A cells (Fig. 1C). Among the 6 breast cancer cell lines, the expression level of ARID1A was the highest in the MCF7 cells and the lowest in the MDA-MB-231 cells. Thus, these 2 cells were selected for use in further experiments. The data on the 5-year survival rate of the breast cancer cases were then acquired, and the results revealed that the overall survival rate of the breast cancer patients with a higher expression of ARID1A was higher than those with a lower expression of ARID1A (Fig. 1D). In addition, as shown in Table I, ARID1A expression was closely related to the TNM stage and the lymph node status of the patients.

Silencing of ARID1A partially reverses the inhibitory effect of 5-FU at various concentrations on cell viability. The MCF7 and MDA-MB-231 cells were selected to further conduct *in vitro* cell experiments. After verifying the successful transfection efficiency of the cells (MCF7 cells transfected with ARID1A siRNA and MDA-MB-231 cells transfected with ARID1A overexpression vector; Fig. 2A-F), it was found that with the increase in the 5-FU concentration (5, 10, 20, 40 and 80 μg/ml), the inhibitory effects of 5-FU on cell viability were enhanced; however, the silencing of ARID1A partially reversed the inhibitory effects of 5-FU, whereas the overexpression of ARIDIA further promoted the inhibitory effects of 5-FU (Fig. 2G and H). RT-qPCR was then performed to examine the effect of 5-FU on ARID1A expression. It was found that 5-FU increased the mRNA level of ARID1A, and with the increase in the 5-FU concentration, the promoting effect of 5-FU was enhanced. However, transfection with ARID1A siRNA or pCMV6-XL4-ARID1A reversed or promoted the effects of 5-FU, respectively (Fig. 2I and J).

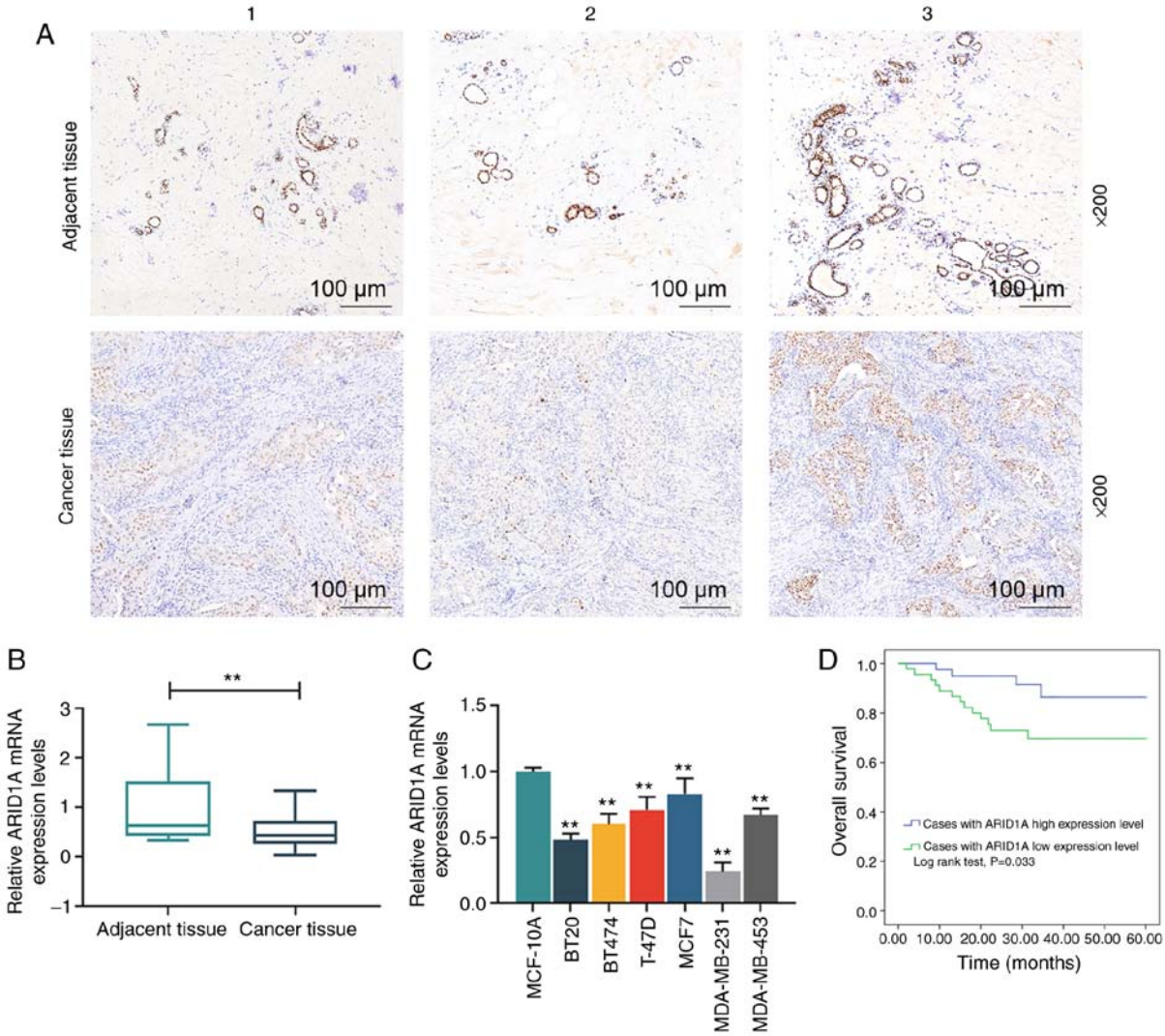

Figure 1. Association of ARID1A expression and breast cancer. (A) Detection of ARID1A expression in breast cancer tissues (n=3) and their matched adjacent tissues (n=3) by immunohistochemistry. The tissue sections are numbered from 1-3. (B) Measurement of the mRNA expression of ARID1A in tissues by RT-qPCR. (C) Detection of the mRNA expression of ARID1A in MCF-10A, BT20, BT474, T-47D, MCF7, MDA-MB-231 and MDA-MB-453 cells by RT-qPCR. (D) Statistical analysis of the relationship between the overall 5-year survival rate and the ARID1A expression level; the overall survival rate was calculated by Kaplan-Meier survival analysis and compared using the log-rank test. Data were obtained from 3 representative experiments and are presented as the means ± standard deviation. The experiment was repeated 3 times (n=3). **P<0.001 vs. adjacent tissue or MCF-10A cells. ARID1A, AT-rich interactive domain 1A.

Silencing of ARID1A suppresses the effects of 5-FU on cells, whereas the overexpression of ARID1A exerts an opposite effect. The concentration of 40 μg/ml 5-FU was then used to treat the cells transfected with ARID1A siRNA or pCMV6-XL4-ARID1A. First, the apoptotic rate of the cells was calculated by flow cytometry. It was found that 5-FU promoted cell apoptosis; however, the silencing of ARID1A partially reversed this effect, whereas transfection with pCMV6-XL4-ARID1A enhanced the effects of 5-FU (Fig. 3A and B). Similar results were obtained with cell cycle analysis: 5-FU exerted an inhibitory effect on the cell cycle at the G0 phase, and the silencing of ARID1A partially reversed this effect. However, the overexpression of ARID1A promoted the effects of 5-FU on the cell cycle (Fig. 3C and D).

A scratch test was also conducted to examine the migration rate of the cells. In this experiment, it was found that the migration distance in the siARID1A group at 24 h was greater than that in the siNC group, and the migration distance in the siNC + 5-FU group was less than that in the siNC group; siARID1A partially reversed the effect of 5-FU on cell migration, whereas the overexpression of ARID1A promoted the effect of 5-FU on cell migration (Fig. 4A and B). In addition, Transwell assay was conducted to detect the invasion rate of the cells. It was found that the silencing of ARID1A promoted cell invasion, whereas 5-FU exerted an opposite effect. The silencing of ARID1A partially reversed the effect of 5-FU on cell invasion, whereas ARID1A overexpression exerted an opposite effect to ARID1A silencing (Fig. 4C and D). Tube formation assay was performed to detect the angiogenesis formation rate of the cells, and the results indicated that cells transfected with ARID1A siRNA exhibited a strong tube formation ability, whereas 5-FU inhibited this ability, and ARID1A overexpression enhanced the effect of 5-FU (Fig. 4E and F).

Silencing of ARID1A promotes the expression of EMT-related proteins, whereas the overexpression of ARID1A exerts an opposite effect. From the results of WB analysis and

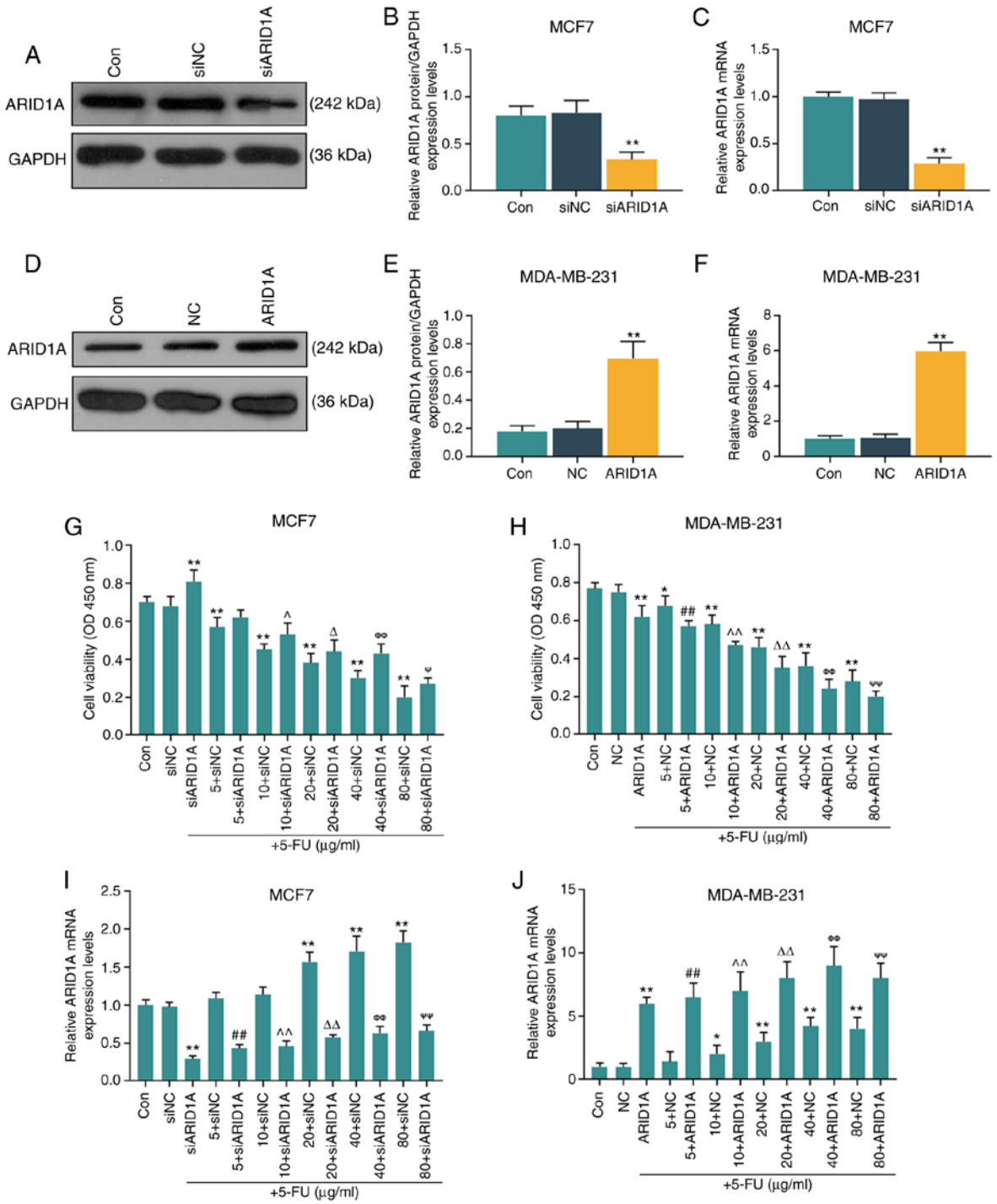

Figure 2. Effects of function of ARID1A on the viability of breast cancer cells treated with 5-FU. (A and B) MCF7 cells were transfected with siARID1A and cultured for 48 h, and the transfection efficiency of siARID1A was detected by WB analysis. (C) The mRNA expression of ARID1A in MCF7 cells was detected by RT-qPCR after the cells were transfected with siARID1A. (D and E) MDA-MB-231 cells were transfected with ARID1A overexpression vector and cultured for 48 h, and the transfection efficiency of ARID1A was detected by WB analysis. (F) The mRNA expression of ARID1A in MDA-MB-231 cells was detected by RT-qPCR after the cells were transfected with ARID1A overexpression vector. (G) The effect of ARID1A silencing on the viability of MCF-7 cells treated with various concentrations of 5-FU (5, 10, 20, 40 and 80 μg/ml) for 24 h was detected by proliferation assay. (H) Effect of ARID1A overexpression on the viability of MDA-MB-231 cells treated with various concentrations of 5-FU (5, 10, 20, 40 and 80 μg/ml) for 24 h was detected by proliferation assay. (I) The mRNA expression of ARID1A in MCF-7 cells treated with various concentrations of 5-FU (5, 10, 20, 40 and 80 μg/ml) and siARID1A was detected by RT-qPCR. (J) The mRNA expression of ARID1A in MDA-MB-231 cells treated with various concentrations of 5-FU (5, 10, 20, 40 and 80 μg/ml) and pCMV6-XL4-ARID1A was detected by RT-qPCR. Data were obtained from 3 representative experiments and are presented as the means ± standard deviation the experiment was repeated 3 times (n=3). *P<0.05, **P<0.001 vs. siNC or NC; $^{\#\#}$P<0.001 vs. 5 + siNC or 5 + NC; $^{\wedge}$P<0.05, $^{\wedge\wedge}$P<0.001 vs. 10 + siNC or 10 + NC; $^{\Delta}$P<0.05, $^{\Delta\Delta}$P<0.001 vs. 20 + siNC or 20 + NC; $^{\Phi\Phi}$P<0.001 vs. 40 + siNC or 40 + NC; $^{\Psi}$P<0.05, $^{\Psi\Psi}$P<0.001 vs. 80 + siNC or 80 + NC. ARID1A, AT-rich interactive domain 1A; 5-FU, 5-fluorouracil; WB analysis, western blot analysis.

RT-qPCR, it was revealed that the cells transfected with ARID1A siRNA exhibited a lower expression of E-cadherin protein and mRNA, and a higher expression of N-cadherin and Vimentin protein and mRNA. 5-FU increased E-cadherin

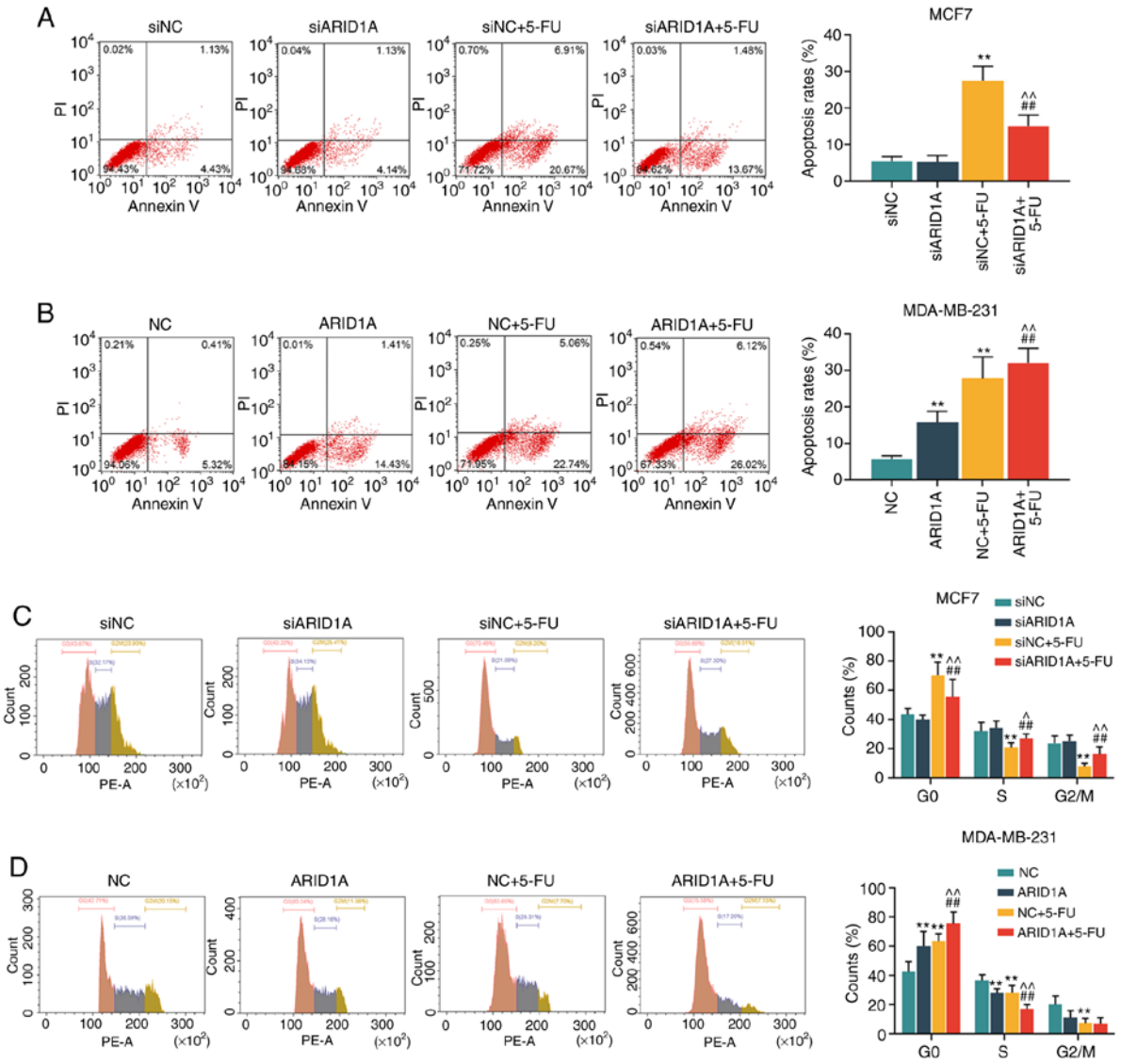

Figure 3. Effects of ARID1A on the apoptosis and cell cycle of breast cancer cells treated with 5-FU. (A and B) The apoptosis of MCF7 and MDA-MB-231 cells following transfection with siARID1A or pCMV6-XL4-ARID1A and treatment with 40 μg/ml 5-FU for 48 h was detected by flow cytometry. (C and D) The cell cycle of MCF7 and MDA-MB-231 cells following transfection with siARID1A or pCMV6-XL4-ARID1A and treatment with 40 μg/ml 5-FU was detected by flow cytometry. Data were obtained from 3 representative experiments and are presented as the means ± standard deviation. The experiment was repeated 3 times (n=3). **P<0.001 vs. siNC or NC; $^{\#\#}$P<0.001 vs. siARID1A or ARID1A; $^{\wedge}$P<0.05, $^{\wedge\wedge}$P<0.001 vs. siNC + 5-FU or NC + 5-FU. ARID1A, AT-rich interactive domain 1A; 5-FU, 5-fluorouracil.

expression and decreased the expression of N-cadherin and Vimentin, whereas the silencing of ARID1A partially reversed the effects of 5-FU (Fig. 5A-C). On the contrary, the cells transfected with pCMV6-XL4-ARID1A exhibited a higher expression of E-cadherin protein and mRNA, and a lower expression of N-cadherin and Vimentin protein and mRNA, and pCMV6-XL4-ARID1A promoted the effects of 5-FU (Fig. 5D-F).

Silencing of ARID1A suppresses the effects of 5-FU on the cell cycle, apoptosis and the expression of angiogenesis-related proteins and mRNAs, whereas the overexpression of ARID1A exerts an opposite effect. From the results of WB analysis and RT-qPCR, it was revealed that the expression levels of ARID1A and Bax were decreased, while those of VEGF, cyclin D1 and Bcl-2 were increased in the siARID1A group; opposite results were observed in the siNC + 5-FU group, while the silencing of ARID1A partially reversed the effects of 5-FU (Fig. 6A-C). On the contrary, the expression levels of ARID1A and Bax were increased, while those of VEGF, cyclin D1 and Bcl-2 were decreased in the ARID1A overexpression group; similar results were observed in the NC + 5-FU group, and ARID1A overexpression promoted the effects of 5-FU (Fig. 6D-F).

Discussion

EMT is a process through which epithelial cells are transformed into mesenchymal cells, characterized by the loss of E-cadherin and the increase in vimentin expression, and this process has been found to be involved in the metastasis of several types of cancer (22-24). The results of the present study suggested that the upregulation of ARID1A expression enhanced the sensitivity of breast cancer cells to 5-FU,

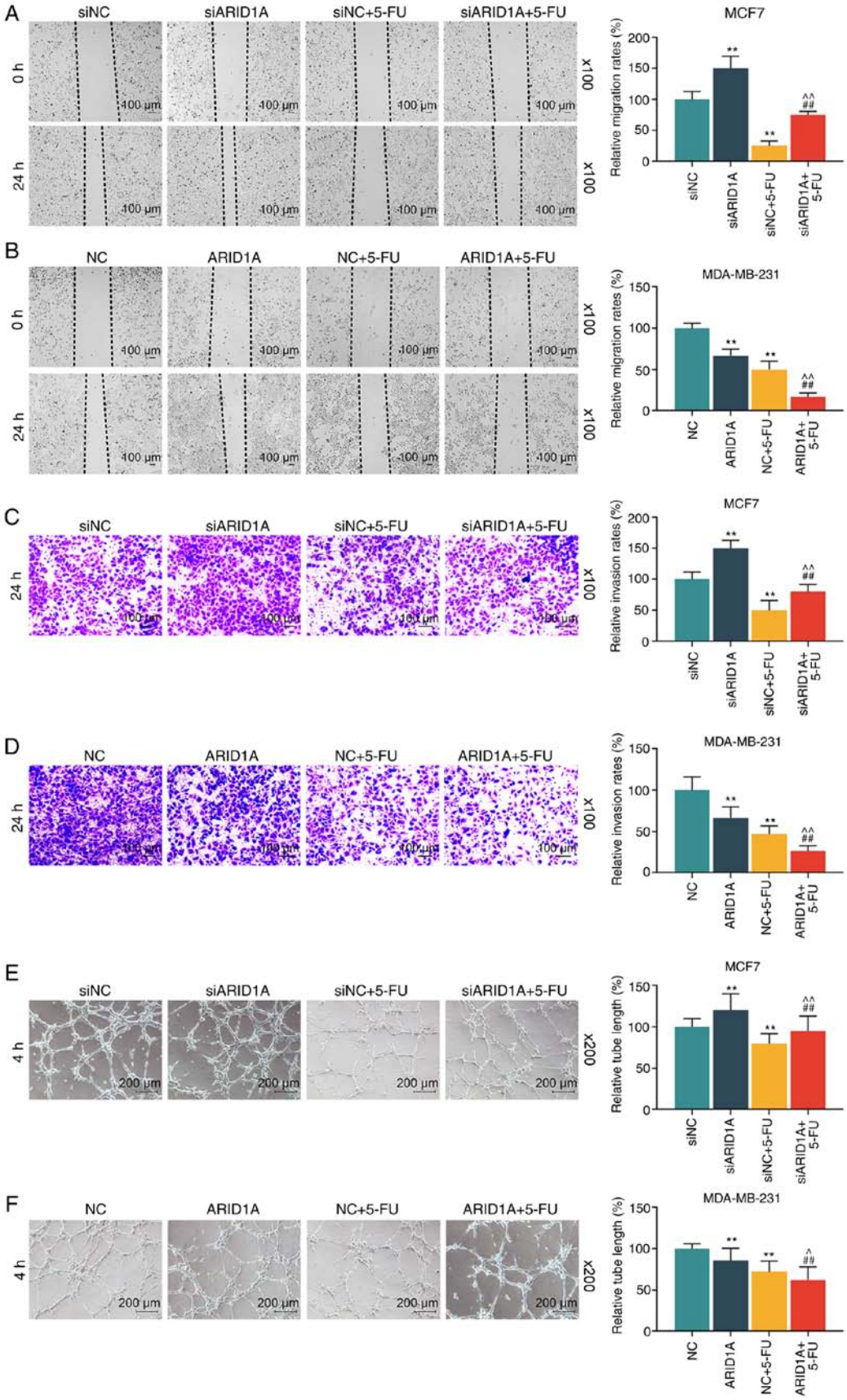

Figure 4. Effets of ARID1A on the migration, invasion and angiogenesis of breast cancer cells treated with 5-FU. (A and B) Detection of the migration rates of MCF7 and MDA-MB-231 cells following transfection with siARID1A or pCMV6-XL4-ARID1A and treatment with 40 μg/ml 5-FU by wound healing migration assay at 0 and 24 h. (C and D) Measurement of the invasion rates of MCF7 and MDA-MB-231 cells following transfection with siARID1A or pCMV6-XL4-ARID1A and treatment with 40 μg/ml 5-FU by invasion assay at 24 h. (E and F) Detection of the angiogenesis formation rates of MCF7 and MDA-MB-231 cells following transfection with siARID1A or pCMV6-XL4-ARID1A and treatment with 40 μg/ml 5-FU by tube formation assay. Data were obtained from 3 representative experiments and are presented as the means ± standard deviation. The experiment was repeated 3 times (n=3). **P<0.001 vs. siNC or NC; $^{\#\#}$P<0.001 vs. siARID1A or ARID1A; $^{\wedge}$P<0.05, $^{\wedge\wedge}$P<0.001 vs. siNC + 5-FU or NC + 5-FU. ARID1A, AT-rich interactive domain 1A; 5-FU, 5-fluorouracil.

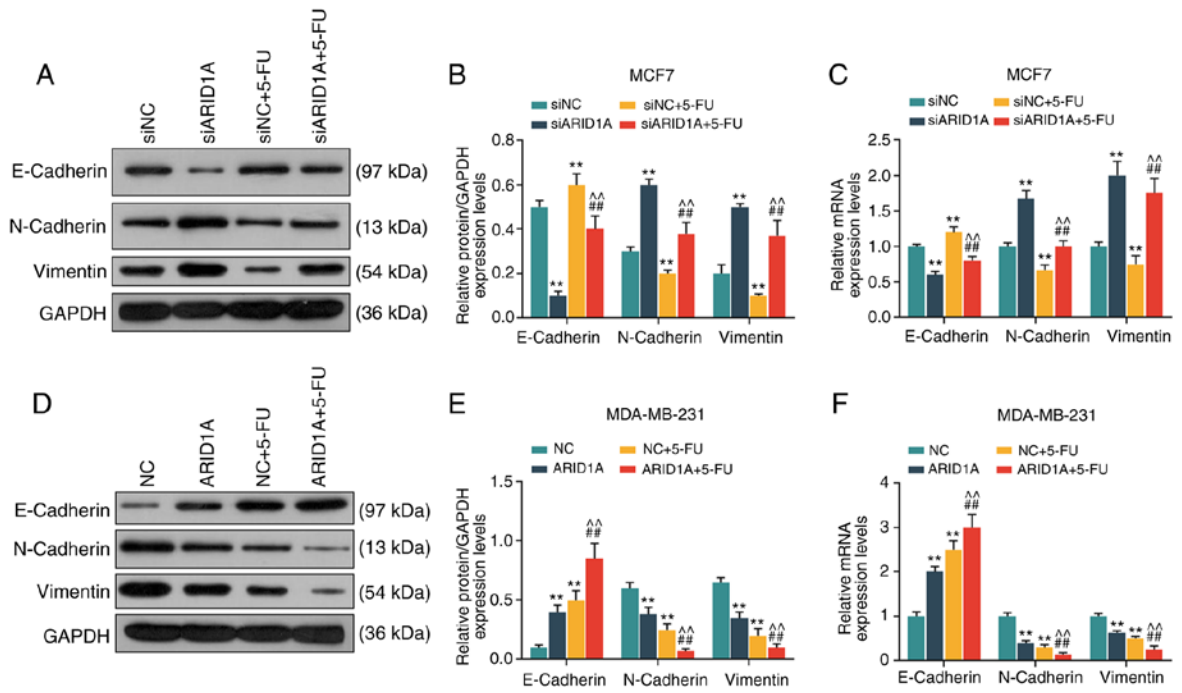

Figure 5. Effects of ARID1A on the expression of EMT-related proteins and mRNAs. (A and B) Detection of the protein expression of E-cadherin, N-cadherin and Vimentin in MCF7 cells by WB analysis. (C) Detection of the mRNA expression of E-cadherin, N-cadherin and Vimentin in MCF7 cells by RT-qPCR. (D and E) Detection of the protein expression of E-cadherin, N-cadherin and Vimentin in MDA-MB-231 cells by WB analysis. (F) The detection of the mRNA expressions of E-cadherin, N-cadherin and Vimentin in MDA-MB-231 cells by RT-qPCR. Data were obtained from 3 representative experiments and are presented as the means ± standard deviation. The experiment was repeated 3 times (n=3). **P<0.001 vs. siNC or NC; $^{\#\#}$P<0.001 vs. siARID1A or ARID1A; $^{\wedge\wedge}$P<0.001 vs. siNC + 5-FU or NC + 5-FU. ARID1A, AT-rich interactive domain 1A; 5-FU, 5-fluorouracil; WB analysis, western blot analysis.

inhibited cell growth, migration and EMT, and promoted cell apoptosis.

5-FU has been widely used as a first-line drug in human cancer chemotherapy. It can target thymidylate synthetase to play an anticancer role by blocking DNA synthesis and interfering in RNA processing. However, the clinical efficacy of 5-FU varies greatly due to chemotherapeutic resistance (25,26). The study by Sagara *et al* in 2016 indicated that 5-FU was a good choice for patients with triple-negative breast cancer with distant metastasis (27). However, drug resistance is an issue worthy of attention in treatment, which was believed to be related to the overexpression of drug efflux transporters or some enzymes or EMT (27). Some researchers have demonstrated that the downregulation of ADAM12-L was helpful in reducing the resistance of breast cancer cells to 5-FU, which was related to the regulation of PI3K/Akt signaling, thus proving that the regulation of ADAM12-L level may have a positive effect on chemotherapy for breast cancer patients in clinical practice (28). Another study reported that the activation of FOXO3a can restore the sensitivity of breast cancer cells to 5-FU (29).

In the present study, the role of ARID1A in 5-FU-treated breast cancer cells was investigated. It was found that the expression of ARID1A was lower in the human cancer tissues than in the normal tissues, and it was also expressed at low levels in breast cancer cell lines. Furthermore, patients with a higher level of ARID1A exhibited a longer survival time, which is consistent with the antitumor effects of ARID1A observed in colon cancer. Mathur *et al* in 2017 found that the loss of ARID1A led to invasive colon adenocarcinoma in mice, and through the detection of some genes, it was found that the regulation of enhancer-mediated gene was probably one of the mechanisms through which ARID1A exerts its anticancer effects on colon cancer (30). Furthermore, Sasaki *et al* in 2019 found that the change in ARID1A can be used as a characteristic of the dual plate malformation type of small cell lung cancer, and also a diagnostic immunohistochemical marker in this disease (31).

Based on previous studies and the present experimental results, the role of ARID1A in the sensitivity to anticancer drugs was further explored. Consistent with findings from previous research that 5-FU inhibits cancer growth (32-34), the results of the present study revealed that 5-FU inhibited the activity of breast cancer cells, by promoting the apoptosis and blocking the cell cycle in the G1 phase. The upregulation of the expression of ARID1A enhanced the effects of 5-FU on the cells. In addition, it was found that 5-FU inhibited the migration, invasion and tube formation of the cells, and the upregulation of ARID1A expression enhanced the effects of 5-FU on the cells, while the downregulation of ARID1A expression exerted an opposite effect to 5-FU. These data suggest that ARID1A plays a role in enhancing the sensitivity of breast cancer cells to 5-FU. Furthermore, the possible mechanisms involved were investigated, and it was found that 5-FU promoted the expression of E-cadherin and inhibited the expression of N-cadherin and Vimentin, whereas the silencing of ARID1A exerted an opposite effect. Cadherin is an important factor in regulating homeostasis. It can transfer adhesion signals into a network of signal effectors and transcription programs, thus regulating cell functions (35). The decreased expression of E-cadherin is a sign of EMT (36). The high expression of N-cadherin is positively associated with

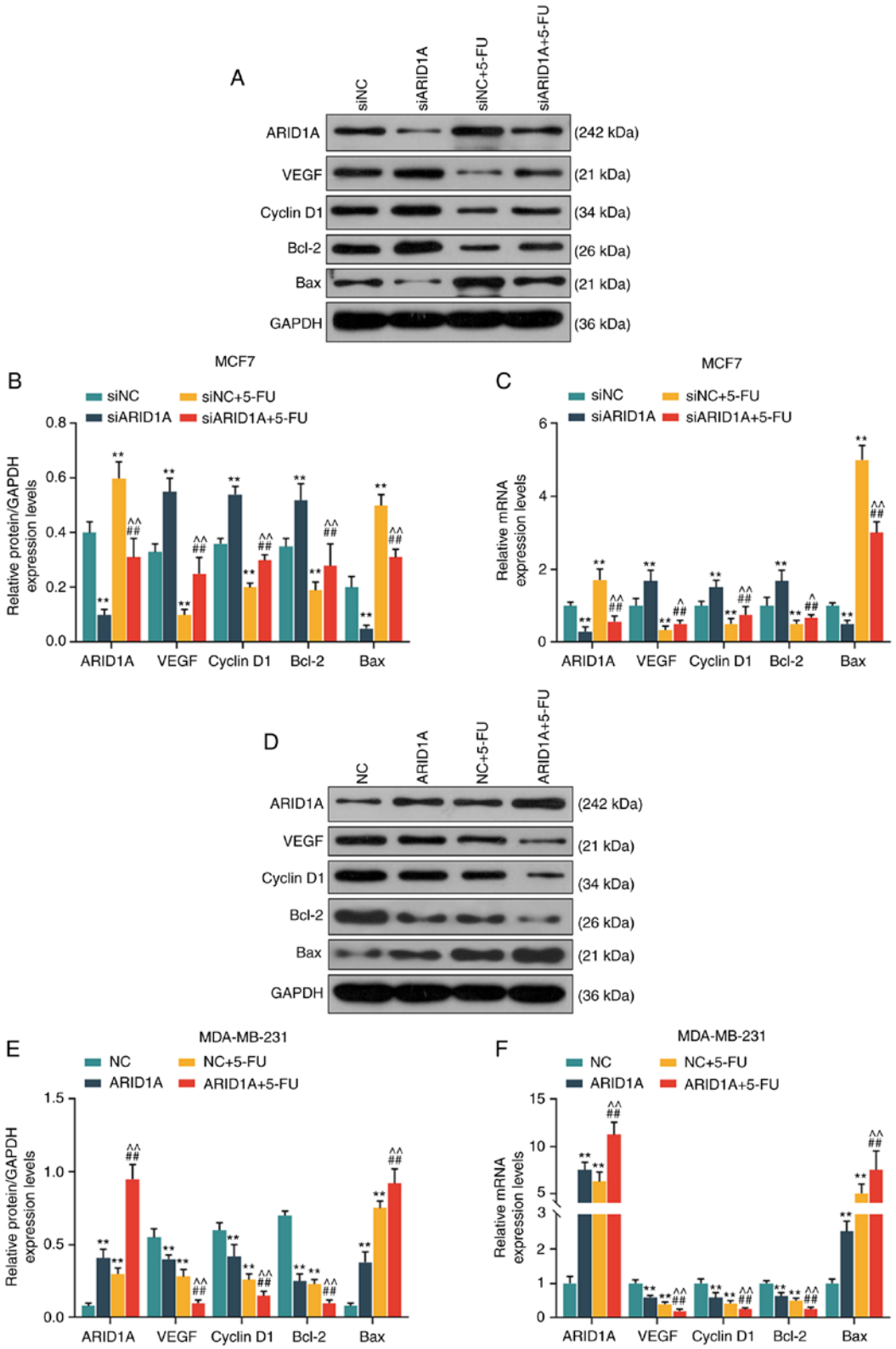

Figure 6. Effects of ARID1A on the cell cycle, apoptosis, and the expression of angiogenesis-related proteins and mRNAs. (A and B) Detection of the protein expression of ARID1A, VEGF, cyclin D1, Bcl-2 and Bax in MCF7 cells by WB analysis. (C) Detection of the mRNA expressions of ARID1A, VEGF, cyclin D1, Bcl-2 and Bax in MCF7 cells by RT-qPCR. (D and E) Detection of the protein expression of ARID1A, VEGF, cyclin D1, Bcl-2 and Bax in MDA-MB-231 cells by WB analysis. (F) Detection of the mRNA expression of ARID1A, VEGF, cyclin D1, Bcl-2 and Bax in MDA-MB-231 cells by RT-qPCR. Data were obtained from 3 representative experiments and are presented as the means ± standard deviation. The experiment was repeated 3 times (n=3). **P<0.001 vs. siNC or NC; $^{\#\#}$P<0.001 vs. siARID1A or ARID1A; $^{\wedge}$P<0.05, $^{\wedge\wedge}$P<0.001 vs. siNC + 5-FU or NC + 5-FU. ARID1A, AT-rich interactive domain 1A; 5-FU, 5-fluorouracil; WB analysis, western blot analysis.

EMT (37). Vimentin is an intermediate silk protein expressed in stromal cells and some ectodermal cells. Its abnormal expression level is related to changes in the cytoskeleton protein structure, and it has the ability to promote cuboidal

epithelial cells to transform into fusiform fibroid cells, and enhance their migratory ability. Therefore, the functions of vimentin are mainly known as maintaining the morphology of cells and organelles, signal transduction, transplantation immunity and apoptosis (38). In the present study, it was found that the upregulation of the expression of ARID1A enhanced the sensitivity of breast cancer cells to 5-FU, thus leading to the inhibition of cell migration and proliferation, which is related to the regulation of the EMT process. Apart from these factors, genes that are related to proliferation, migration, invasion and tube formation, such as VEGF, cyclin D1, Bcl-2 and Bax, were also influenced by 5-FU and the effect of 5-FU on these genes were partially reversed by ARID1A silencing.

On the whole, the loss-of-function mutation of ARID1A often occurs in breast cancer patients. The present study demonstrated that the upregulation of the expression of ARID1A can enhance the sensitivity of breast cancer cells to 5-FU, inhibit cell growth, migration and EMT, and promote cell apoptosis. However, there are also some limitations to the present study; for example, in the future, animal models are required to further verify the effects of ARID1A on breast cancer models to 5-FU, and further experiments and test indicators are required to clarify the mechanisms of action of ARID1A.

In conclusion, the present study demonstrates that ARID1A plays an anticancer role in breast cancer and enhances the sensitivity of breast cancer cells to 5-FU. These findings may provide a novel treatment strategy for breast cancer.

Acknowledgements

Not applicable.

Funding

No funding was received.

Availability of data and materials

The datasets used and/or analyzed during the current study are available from the corresponding author on reasonable request.

Authors' contributions

TW and XG made substantial contributions to the conception and design of the study. KZ, TJ, SG, PL, XZ and XS were involved in data acquisition, data analysis and interpretation. TW and XG were involved in the drafting of the article or critically revising it for important intellectual content. All authors gave the final approval of the final version of the article to be published and all authors agree to be accountable for all aspects of the work in ensuring that questions related to the accuracy or integrity of the work are appropriately investigated and resolved.

Ethics approval and consent to participate

All procedures performed involving human participants were in accordance with the ethical standards of the institutional and/or national research committee and with the 1964 Helsinki declaration and its later amendments or comparable ethical standards. Approval for the study was obtained from the Dongzhimen Hospital Ethics Committee (approval no. CH201309270). Written informed consent was obtained from each patient. No animals are involved in the present study.

Patient consent for publication

Not applicable.

Competing interests

The authors declare that they have no competing interests.

References

1. Liang HF, Zhang XZ, Liu BG, Jia GT and Li WL: Circular RNA circ-ABCB10 promotes breast cancer proliferation and progression through sponging miR-1271. Am J Cancer Res 7: 1566-1576, 2017.
2. Balekouzou A, Yin P, Pamatika CM, Bishwajit G, Nambei SW, Djeintote M, Ouansaba BE, Shu C, Yin M, Fu Z, *et al*: Epidemiology of breast cancer: Retrospective study in the Central African Republic. BMC Public Health 16: 1230, 2016.
3. Calado A, Neves PM, Santos T and Ravasco P: The effect of flaxseed in breast cancer: A literature review. Front Nutr 5: 4, 2018.
4. Yates LR, Knappskog S, Wedge D, Farmery JHR, Gonzalez S, Martincorena I, Alexandrov LB, Van Loo P, Haugland HK, Lilleng PK, *et al*: Genomic evolution of breast cancer metastasis and relapse. Cancer Cell 32: 169-184.e7, 2017.
5. Goodarzi H, Nguyen HCB, Zhang S, Dill BD, Molina H and Tavazoie SF: Modulated expression of specific tRNAs drives gene expression and cancer progression. Cell 165: 1416-1427, 2016.
6. Ketterer S, Gomez-Auli A, Hillebrand LE, Petrera A, Ketscher A and Reinheckel T: Inherited diseases caused by mutations in cathepsin protease genes. FEBS J 284: 1437-1454, 2017.
7. Butchbach ME: Copy number variations in the survival motor neuron genes: Implications for spinal muscular atrophy and other neurodegenerative diseases. Front Mol Biosci 3: 7, 2016.
8. Jensen SM, Kumar S, Chowdhury A, Castro N, Shih J, Salomon DS and Stetler-Stevenson WG: TIMP-2 inhibits triple negative breast cancer growth and metastasis through EMT suppression and promotion of vascular normalization. FASEB J 32: 678.672, 2018.
9. Raoof S, Mulford IJ, Frisco-Cabanos H, Nangia V, Timonina D, Labrot E, Hafeez N, Bilton SJ, Drier Y, Ji F, *et al*: Targeting FGFR overcomes EMT-mediated resistance in EGFR mutant non-small cell lung cancer. Oncogene 38: 6399-6413, 2019.
10. Li C, Wang J, Kong J, Tang J, Wu Y, Xu E, Zhang H and Lai M: GDF15 promotes EMT and metastasis in colorectal cancer. Oncotarget 7: 860-872, 2016.
11. Chunder N, Mandal S, Basu D, Roy A, Roychoudhury S and Panda CK: Deletion mapping of chromosome 1 in early onset and late onset breast tumors-a comparative study in eastern India. Pathol Res Pract 199: 313-321, 2003.
12. Bitler BG, Wu S, Park PH, Hai Y, Aird KM, Wang Y, Zhai Y, Kossenkov AV, Vara-Ailor A, Rauscher FJ III, *et al*: ARID1A-mutated ovarian cancers depend on HDAC6 activity. Nat Cell Biol 19: 962-973, 2017.
13. Takeda T, Banno K, Okawa R, Yanokura M, Iijima M, Irie-Kunitomi H, Nakamura K, Iida M, Adachi M, Umene K, *et al*: ARID1A gene mutation in ovarian and endometrial cancers (Review). Oncol Rep 35: 607-613, 2016.
14. Wang K, Kan J, Yuen ST, Shi ST, Chu KM, Law S, Chan TL, Kan Z, Chan AS, Tsui WY, *et al*: Exome sequencing identifies frequent mutation of ARID1A in molecular subtypes of gastric cancer. Nat Genet 43: 1219-1223, 2011.
15. Shain AH, Giacomini CP, Matsukuma K, Karikari CA, Bashyam MD, Hidalgo M, Maitra A and Pollack JR: Convergent structural alterations define SWItch/Sucrose NonFermentable (SWI/SNF) chromatin remodeler as a central tumor suppressive complex in pancreatic cancer. Proc Natl Acad Sci USA 109: E252-E259, 2012.

16. Li L, Li M, Jiang Z and Wang X: ARID1A mutations are associated with increased immune activity in gastrointestinal cancer. Cells 8: 678, 2019.
17. Takao C, Morikawa A, Ohkubo H, Kito Y, Saigo C, Sakuratani T, Futamura M, Takeuchi T and Yoshida K: Downregulation of ARID1A, a component of the SWI/SNF chromatin remodeling complex, in breast cancer. J Cancer 8: 1-8, 2017.
18. Zhang Y and Weinberg RA: Epithelial-to-mesenchymal transition in cancer: Complexity and opportunities. Front Med 12: 361-373, 2018.
19. Somsuan K, Peerapen P, Boonmark W, Plumworasawat S, Samol R, Sakulsak N and Thongboonkerd V: ARID1A knockdown triggers epithelial-mesenchymal transition and carcinogenesis features of renal cells: Role in renal cell carcinoma. FASEB J 33: 12226-12239, 2019.
20. Wilson MR, Reske JJ, Holladay J, Wilber GE, Rhodes M, Koeman J, Adams M, Johnson B, Su RW, Joshi NR, *et al*: ARID1A and PI3-kinase pathway mutations in the endometrium drive epithelial transdifferentiation and collective invasion. Nat Commun 10: 3554, 2019.
21. Livak KJ and Schmittgen TD: Analysis of relative gene expression data using real-time quantitative PCR and the 2(-Delta Delta C(T)) method. Methods 25: 402-408, 2001.
22. Rokavec M, Kaller M, Horst D and Hermeking H: Pan-cancer EMT-signature identifies RBM47 down-regulation during colorectal cancer progression. Sci Rep 7: 4687, 2017.
23. Das V, Bhattacharya S, Chikkaputtaiah C, Hazra S and Pal M: The basics of epithelial-mesenchymal transition (EMT): A study from a structure, dynamics, and functional perspective. J Cell Physiol: Feb 5, 2019 (Epub ahead of print). doi: 10.1002/jcp.28160.
24. Koeck S, Amann A, Huber JM, Gamerith G, Hilbe W and Zwierzina H: The impact of metformin and salinomycin on transforming growth factor β-induced epithelial-to-mesenchymal transition in non-small cell lung cancer cell lines. Oncol Lett 11: 2946-2952, 2016.
25. Liu H, Yin Y, Hu Y, Feng Y, Bian Z, Yao S, Li M, You Q and Huang Z: miR-139-5p sensitizes colorectal cancer cells to 5-fluorouracil by targeting NOTCH-1. Pathol Res Pract 212: 643-649, 2016.
26. He L, Zhu H, Zhou S, Wu T, Wu H, Yang H, Mao H, SekharKathera C, Janardhan A, Edick AM, *et al*: Wnt pathway is involved in 5-FU drug resistance of colorectal cancer cells. Exp Mol Med 50: 101, 2018.
27. Sagara A, Igarashi K, Otsuka M, Karasawa T, Gotoh N, Narita M, Kuzumaki N, Narita M and Kato Y: Intrinsic resistance to 5-fluorouracil in a brain metastatic variant of human breast cancer cell line, MDA-MB-231BR. PLoS One 11: e0164250, 2016.
28. Wang X, Wang Y, Gu J, Zhou D, He Z, Wang X and Ferrone S: ADAM12-L confers acquired 5-Fluorouracil resistance in breast cancer cells. Sci Rep 7: 9687, 2017.
29. Song Y, Lu M, Qiu H, Yin J, Luo K, Zhang Z, Jia X, Zheng G, Liu H and He Z: Activation of FOXO3a reverses 5-Fluorouracil resistance in human breast cancer cells. Exp Mol Pathol 105: 57-62, 2018.
30. Mathur R, Alver BH, San Roman AK, Wilson BG, Wang X, Agoston AT, Park PJ, Shivdasani RA and Roberts CW: ARID1A loss impairs enhancer-mediated gene regulation and drives colon cancer in mice. Nat Genet 49: 296-302, 2017.
31. Sasaki M, Sato Y and Nakanuma Y: Cholangiolocellular carcinoma with 'Ductal plate malformation' pattern may be characterized by ARID1A genetic alterations. Am J Surg Pathol 43: 352-360, 2019.
32. Wang X, Wang X, Gu J, Zhou M, He Z, Wang X and Ferrone S: Overexpression of miR-489 enhances efficacy of 5-fluorouracil-based treatment in breast cancer stem cells by targeting XIAP. Oncotarget 8: 113837-113846, 2017.
33. Hashemi-Moghaddam H, Kazemi-Bagsangani S, Jamili M and Zavareh S: Evaluation of magnetic nanoparticles coated by 5-fluorouracil imprinted polymer for controlled drug delivery in mouse breast cancer model. Int J Pharm 497: 228-238, 2016.
34. Gao F, Yu X, Meng R, Wang J and Jia L: STARD13 is positively correlated with good prognosis and enhances 5-FU sensitivity via suppressing cancer stemness in hepatocellular carcinoma cells. Onco Targets Ther 11: 5371-5381, 2018.
35. Bruner HC and Derksen PW: Loss of E-cadherin-dependent cell-cell adhesion and the development and progression of cancer. Cold Spring Harb Perspect Biol 10: a029330, 2018.
36. Ogasawara N, Kudo T, Sato M, Kawasaki Y, Yonezawa S, Takahashi S, Miyagi Y, Natori Y and Sugiyama A: Reduction of membrane protein CRIM1 decreases E-cadherin and increases claudin-1 and MMPs, enhancing the migration and invasion of renal carcinoma cells. Biol Pharm Bull 41: 604-611, 2018.
37. Tanaka T, Goto K and Iino M: Sec8 modulates TGF-β induced EMT by controlling N-cadherin via regulation of Smad3/4. Cell Signal 29: 115-126, 2017.
38. Liao S, Yu C, Liu H, Zhang C, Li Y and Zhong X: Long non-coding RNA H19 promotes the proliferation and invasion of lung cancer cells and regulates the expression of E-cadherin, N-cadherin, and vimentin. Onco Targets Ther 12: 4099-4107, 2019.